

# VALIDATION PROCESS FOR COMPUTATIONAL MODEL OF FULL-SCALE SEGMENT FOR DESIGN OF COMPOSITE FOOTBRIDGE

Tomasz Ferenc

Tomasz Mikulski

Gdansk University of Technology, Poland

## ABSTRACT

*Experimental tests and numerical simulations of a full-scale segment of a foot and cycle bridge made of polymer composites are presented in the paper. The analysed structure is made of sandwich panels, which consist of glass fibre reinforced polymer (GFRP) multi-layered laminate faces and a PET foam (obtained from recycling) core. The dimensions of the segment cross-section are the same as for the target footbridge; however, span length was reduced to 3 m.*

*The experimental tests were conducted in a laboratory of the Faculty of Ocean Engineering and Ship Technology at Gdansk University of Technology. A single vertical force was generated by a hydraulic cylinder and was applied to the platform of the structure. The experimental tests were supported by numerical analyses performed in Femap with NX Nastran software by means of the finite element method (FEM). Results obtained in the computational model were compared with results from experiments. Thus, the numerical model was validated and the obtained conclusions were used in the next step of the design process of a composite footbridge with a span length of 14.5 m.*

**Keywords:** Validation, numerical modelling, sandwich structure, polymer composites, GFRP laminates

## INTRODUCTION

The design process of every engineering structure is realized in stages: from conception, through design assumption formulation, to calculations, technical drawings, and technological process development. A properly carried out process is the basis for efficient investment implementation. This process is even more complicated when the structure is innovative or unusual. The purpose of experimental studies, in addition to obtaining information about the behaviour of the structure itself, is predominantly to validate the numerical model [1]. This process is about checking and possibly modifying the parameters describing a mathematical model representing a real structure to provide results similar to reality with sufficient accuracy [10, 11, 13]. Measured values (like displacement or strain) at various points in the real structure are checked and compared with those obtained from the numerical model

at the beginning for the initial values of parameters. When results received from this comparison seem to be unsatisfactory, parameters of the numerical model have to be modified. This process is extensively used in every field of engineering – from the automotive industry, through the aviation and maritime industries [17, 18], to civil engineering [12, 14]. All abovementioned industries have in common one more thing: the rapidly increasing popularity of the usage of composite materials [7].

The paper consists of an analysis of a 3-m-long segment of a fully composite footbridge which is assumed to be a sandwich and shell structure. This kind of structure is very often used in the maritime industry, especially while constructing hulls, masts, or other elements of ships or yachts. Nowadays, a typical yacht or catamaran hull is made from polymer composite materials and works as a shell. Moreover, it is a sandwich structure which increases its flexural stiffness by increasing its thickness. Hence, the capacity of the structure is increased.



Fig. 1. Examples of a yacht and catamaran made from composites (<https://sunreef-yachts.com>)

Fig. 1a presents a luxury yacht from Sunreef Yachts, Gdańsk, while Fig. 1b shows an A-class Exploder catamaran produced by Jakub Kopyłowicz, Tczew (Poland).

A simplified diagram of the design process of a composite pedestrian bridge [6] is shown in Fig. 2, in which one of the stages was validation of the numerical model of a 3-m-long segment with a full-sized cross-section. After the initial concepts (a) the numerical model was created and on this basis (1), the real structure of the segment was designed (b) and then manufactured (c). Based on the numerical model, an experimental test program was prepared (2). Results obtained from experiments allowed us to conduct the validation (3) of the numerical model of the segment. Therefore, the conclusions allowed us to create a numerical model of the target footbridge (4) and then to conduct numerical simulations to design the target structure (d).

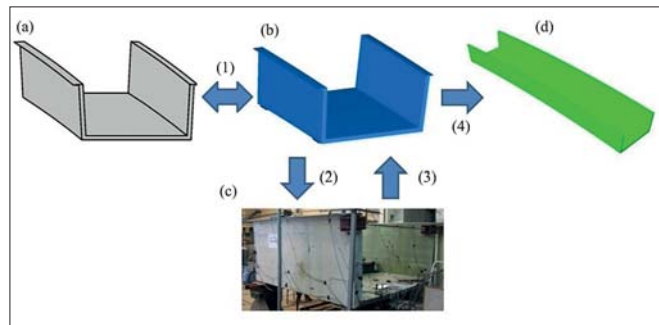


Fig. 2. A simplified diagram of the design process of a composite pedestrian bridge

## DESCRIPTION OF SEGMENT

The analysed segment has the same cross-section dimensions as the target footbridge, with the exception that its length is reduced to 3 m. The usable width is 2.5 m and the handrail height is 1.3 m (Fig. 3). Hence, the legal and standard requirements for pedestrian and cycle traffic are met. The target footbridge will be erected over a two-lane

motorway or railroad. The shape of the cross-section was assumed to be U-shaped; thus, the structure is a shell type.

The segment, as well as the target footbridge, was assumed to be made only from composite materials. The first approach was to build walls and a platform as a multi-layered laminate. However, the numerical analysis showed a lack of capacity for such a structure. Thus, to increase the stiffness of elements of the segment, the walls and platform were assumed to be a sandwich structure that could to a greater extent take advantage of the benefits of high-strength laminate.

The faces of the sandwich structure (Fig. 4) of the segment were built using multi-layered glass fibre reinforced polymer GFRP laminate. Two types of glass-stitched fabrics were used, denoted as BAT and GBX, with fibre orientations of

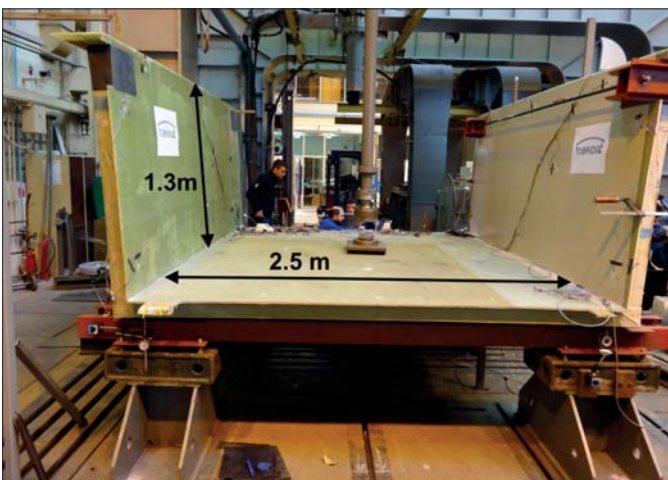


Fig. 3. Geometry of analysed segment

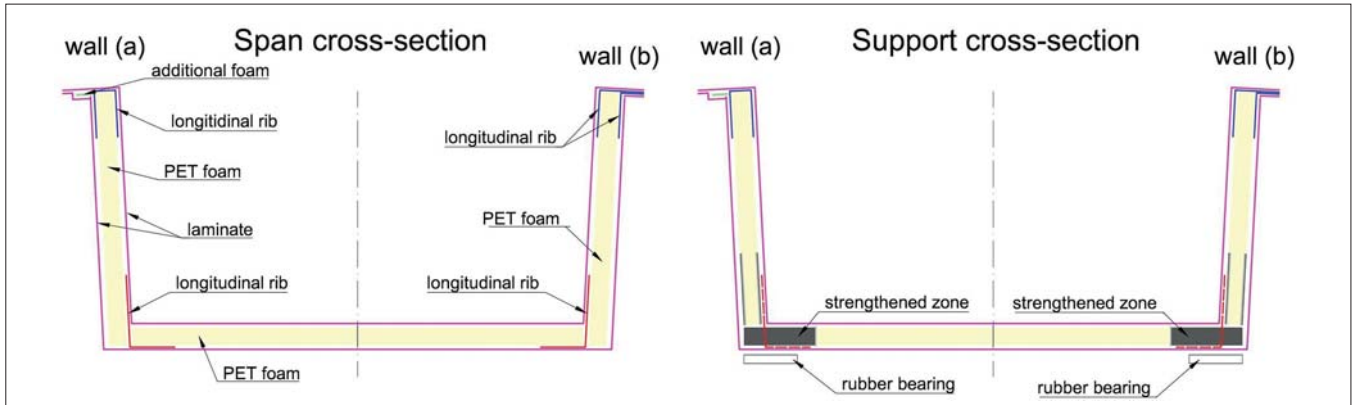


Fig. 4. Span and support cross-section of segment (after [2])

[0/90] and [+45/-45], respectively. The density of both fabrics is 800 g/m<sup>2</sup>. The laminate matrix is constituted of polymer and vinyl ester resin with an additional component that makes it flame retardant. The stack sequence of laminate in the whole structure is constant, as is its thickness. Both faces, in the walls and platform, have six layers [BAT/GBX/BAT/BAT/GBX/BAT] and a total thickness of 3.978 mm which is the result of the multiplication of the thickness of a single laminate layer which is 0.663 mm. The density of the laminates is 1.71 g/cm<sup>3</sup>. In specific areas the stack sequence was reinforced by adding extra longitudinal and transverse ribs. Longitudinal ribs were added near handrails and near the connection of walls and platform for two reasons. First, for technological considerations, these were added between blocks of PET foam. The second reason was to increase the stiffness of the structure. Additionally, transverse ribs were used mainly because of the technology. The core is made of PET foam produced in blocks with a density of 100 kg/m<sup>3</sup> obtained from the recycling of plastic bottles. The thickness of the core is constant in the walls and platform at 10 cm. Furthermore, instead of typical PET foam, strengthened elements were used around the support zone (Fig. 4b).

Material parameters of laminates were determined within the project (by the Military University of Technology in Warsaw [3] and the Gdansk University of Technology [15]) and are listed in Table 1. Material parameters for PET foam were taken from the producer and are as follows: elastic modulus  $E = 70$  MPa and Poisson's ratio  $\nu = 0.4$ . Near the support zone, instead of PET foam, strengthened elements were used in the form of a composite block; material properties are listed in Table 2.

The segment was manufactured using an infusion process that involved placing dry constructive elements, like stitched fabrics and PET foam, on a mould, and then covering everything with a bag and, finally, by applying liquid resins under pressure. The production of the segment was conducted under the same conditions as the target footbridge, which was itself a manufacturing test.

The segment was supported on four rectangular rubber bearings with dimensions of 30x30x3 cm. The material parameters of the bearings were investigated in compressive tests – the stiffness modulus is  $E = 12.58$  MPa and Poisson's

ratio is  $\nu = 0.48$ . Although the total length of the segment is 3 m, the theoretical length was assumed to be 2.5 m.

## EXPERIMENT

Experiments were conducted in the laboratory of the Faculty of Ocean Engineering and Ship Technology at Gdansk University of Technology. Although several load schemes were used, including static [2], dynamic, and cyclic tests [16], one was ultimately chosen as the most representative scheme for the validation process of the numerical model. In that scheme, a single vertical force was generated by a hydraulic cylinder and was applied on the platform of the segment. The level of force was assessed before conducting the experiment to avoid micro-cracking in laminates and destruction of the PET foam. Hence, a single force of 50 kN was applied at the middle of the platforms' width and span lengths (Fig. 5). That load was established at a level that causes stress of about

Tab. 1. Material parameters of single GFRP ply [2]

Parameter	Description	Value	Unit
$E_1$   $E_2$	longitudinal (1) and transverse (2) elastic moduli	23.4	[GPa]
$\nu_{12}$	Poisson's ratio	0.153	[-]
$G_{12}$	in-plane shear modulus	3.52	[GPa]
$G_{13}$   $G_{23}$	transverse shear moduli	1.36	[GPa]

Tab. 2. Material parameters of single composite blocks [2]

Parameter	Description	Value	Unit
$E_1$   $E_2$	longitudinal (1) and transverse (2) elastic moduli	8.25	[GPa]
$E_2$	transverse (3) elastic modulus	4.15	[GPa]
$\nu_{12}$	in-plane Poisson's ratio	0.39	[-]
$\nu_{13}$	transverse (23) Poisson's ratio	0.235	[-]
$\nu_{31}$	transverse (31) Poisson's ratio	0.118	[-]
$G_{12}$	in-plane shear modulus	3.04	[GPa]
$G_{13}$   $G_{23}$	transverse shear moduli	3.1	[GPa]



Fig. 5. Force applied at the middle of platform's width and length



Fig. 6. Sensors used during experiment: (a) strain gauge, (b) displacement sensor, (c) dial gauge with rubber bearing

20% of the strength of the laminate, computed according to the Tsai–Wu criterion.

During the experiment, several measurement instruments were used to measure segment parameters. To obtain strain, 15 strain gauges (T) were installed (Fig. 6a), to measure displacement, seven displacement sensors (U) were used (Fig. 6b) and to measure displacement around the support zone, four dial gauges (O) were attached – one next to each rubber bearing (Fig. 6c).

To specify the location of each sensor (Fig. 7), preliminary calculations were carried out on the initial numerical model. The measuring points were chosen in order to obtain a high value of the measured parameter.

## NUMERICAL MODEL OF THE SEGMENT

A numerical model of the segment was created and analysed using Femap (with NX Nastran) environment by means of the finite element method (FEM). Geometry was assessed according to the dimensions of structure. Two kinds of finite elements were used – laminated faces of the sandwich were modelled using four node shell elements by means of the equivalent single layer (ESL) approach with first order shear deformation theory (FOSD) while a PET foam core was modelled as eight node solid elements. Both types of elements have linear-shaped functions with full integration. Material parameters of elements, laminate, PET foam, composite

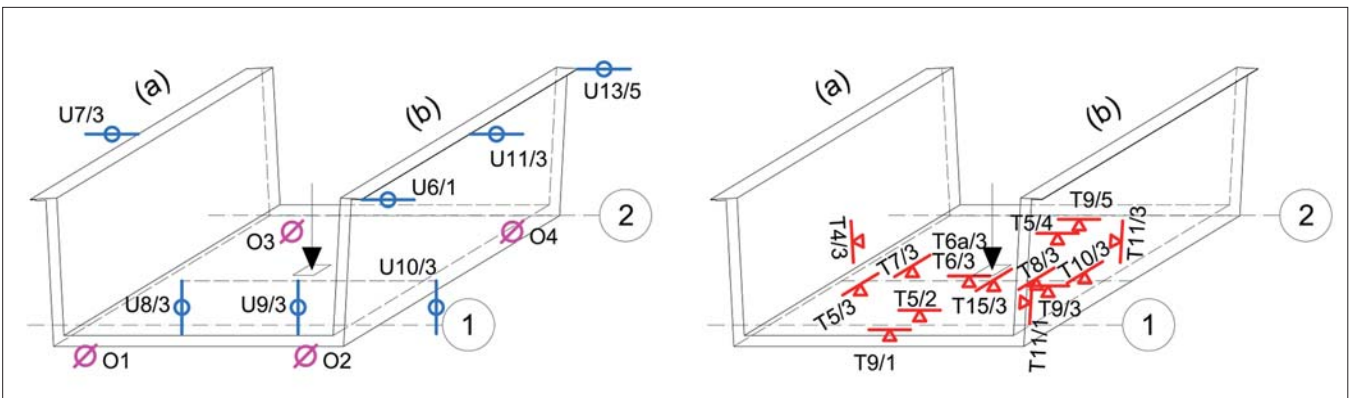


Fig. 7. Location of sensors during experiment

blocks, and rubber bearings were assumed according to Table 1, Table 2, and the information given before.

A regular mesh was created which assumed the distance between nodes at the lever was about 25 mm. An overall view of the model is presented in Fig. 8a. Additionally, details of the load applied at the middle of the platform are shown in Fig. 8b. The load was applied through a stiff element of area 30x30 cm. Moreover, Fig. 8c presents one of four rubber bearings with FEM discretization. On the upper side, bearings are merged with the segment, while on the bottom side the translations in all three directions are blocked.

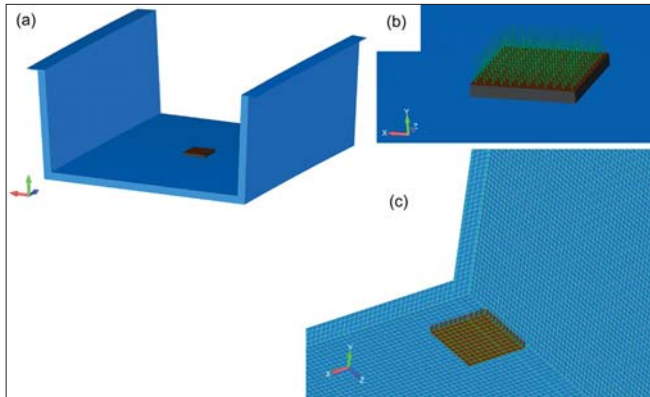


Fig. 8. Computational model: (a) overall view, (b) applied force, (c) rubber bearing

Tab. 3. Comparison of values obtained at measuring points in experiment and initial model

Sensor	Experiment	Model before validation	Relative error
Strain [ $\mu\text{m}/\text{m}$ ]			
T9/1	668	336	-98.8%
T5/2	605	519	-16.6%
T5/3	121	201	39.8%
T6/3	1240	1834	32.4%
T8/3	167	583	71.4%
T9/3	118	128	7.8%
T15/3	835	1137	26.6%
T5/4	640	513	-24.8%
T9/5	585	335	-74.6%
Displacement [mm]			
U7/3	-11.10	-5.27	-110.6%
U8/3	1.96	0.48	-308.3%
U9/3	14.60	17.27	15.5%
U10/3	1.42	0.47	-202.1%
U11/3	-11.21	-5.33	-110.3%

## VALIDATION PROCESS AND RESULTS COMPARISON

Values of various parameters obtained from experiments were compared with those from the initial numerical model and are listed in Table 3. Strain values and displacement were measured at nine and five representative points, respectively. The relative error reached a maximum of 74% taking into account measure strain (in sensor T9/5) and 308% considering displacement in inductive sensor U8/3.

Values of various parameters seemed to be unsatisfactory; thus, parameters of the numerical model had to be modified. Three main reasons that caused these differences were discerned.

Firstly, the dimensions of the real segment were slightly different than assumed. Besides conducting experiments, manufacturing of the segment itself was also a technological test because it was the first full-scale element produced during the FOBRIDGE project. Therefore, some mistakes could not be avoided: e.g., the foam blocks moved lengthwise and thus the segment was extended by 10 cm. That had an impact of increasing the assumed weight. Hence, the geometry of the numerical model had to be updated.

Furthermore, full contact between the segment and the squared rubber bearing was assumed, with merged nodes. This did not take place in the real construction due to the possibility of peeling. Moreover, at the stage of assumptions of the research program and preliminary calculations, the contact surface was to be square, like the shape of the rubber bearings. However, the real contact surfaces we encountered during experiments (presented in Fig. 9) are slightly different. Grey areas represent contact surface, while white areas show no-contact fields. Due to the play between the segment and the rubber bearings, modifications for the rubber bearing material parameters were conducted. In order to achieve greater accuracy, displacements obtained from dial gauges located around support zones (O1, O2, O3, and O4) were compared with those obtained from numerical simulations and then stiffness moduli of rubber bearings were updated. The equivalent bearing parameters recorded this way are summarized in Table 4. Additionally, all bearings were assumed to be non-sliding.

Tab. 4. Updated elastic moduli of rubber bearings [2]

Sensor	Displacement in experim. [mm]	Updated elastic modulus [MPa]	Displacement in model [mm]
O1	1.36	0.63	1.41
O2	1.40	0.64	1.40
O3	1.16	0.7	1.23
O4	0.99	0.85	1.03

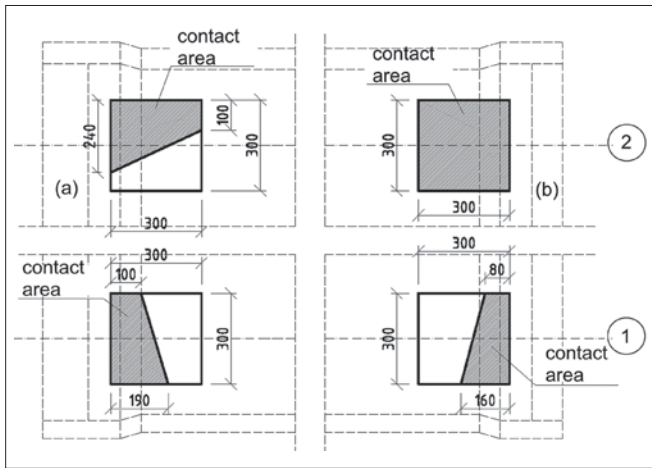


Fig. 9. The real contact surface between segment and bearings

In addition, as mentioned before, the segment is a sandwich structure with laminate inner and outer faces and a PET foam core. Moreover, the construction also consists of longitudinal and transverse ribs. Generally, longitudinal ribs are added to provide higher stiffness in specific segment areas (more layers of laminates), while transverse ones are used due to requirements of the production technology. At the stage of preliminary calculations, the extra margin of the ribs, presented in Fig. 10, were not taken into account. In fact, the stacking of the structure laminate was enriched by additional layers.

Finally, after the abovementioned modifications of the computational model, it consisted of 155779 nodes and 227082 elements in total. The results obtained from the numerical analysis and experiment were compared again. This comparison showed increased agreement of results, which means that accuracy also increased. Table 5 presents a list of values obtained from the numerical model analysis after the validation process and experiment were conducted.

The relative error, taking into account strain, reaches a maximum of 30% in sensor T15/3, but mostly it is much

Tab. 5. Comparison of values obtained at measurement points in experiment and model after validation [2]

Sensor	Experiment	Model after validation	Relative error
Strain [ $\mu\text{m}/\text{m}$ ]			
T9/1	668	545	-22.6%
T5/2	605	627	3.6%
T5/3	121	112	-7.6%
T6/3	1240	1451	14.6%
T8/3	167	213	21.6%
T9/3	118	113	-4.0%
T15/3	835	641	-30.3%
T5/4	640	622	-2.8%
T9/5	585	549	-6.5%
Displacement [mm]			
U7/3	-11.10	-12.6	11.9%
U8/3	1.96	0.98	-99.5%
U9/3	14.60	16.27	10.3%
U10/3	1.42	1	-41.5%
U11/3	-11.21	-12.86	12.8%

smaller. Considering displacement, maximum relative error is about 100%, but here measured values are relatively small; thus, even a little variation causes high error. For the more representative points – U7/1, U9/3, and U11/3 – relative error is about 10%. Additionally, Fig. 11 presents a graphical comparison of obtained values which can be considered a good confirmation that the agreement of the results increased after the mentioned modifications.

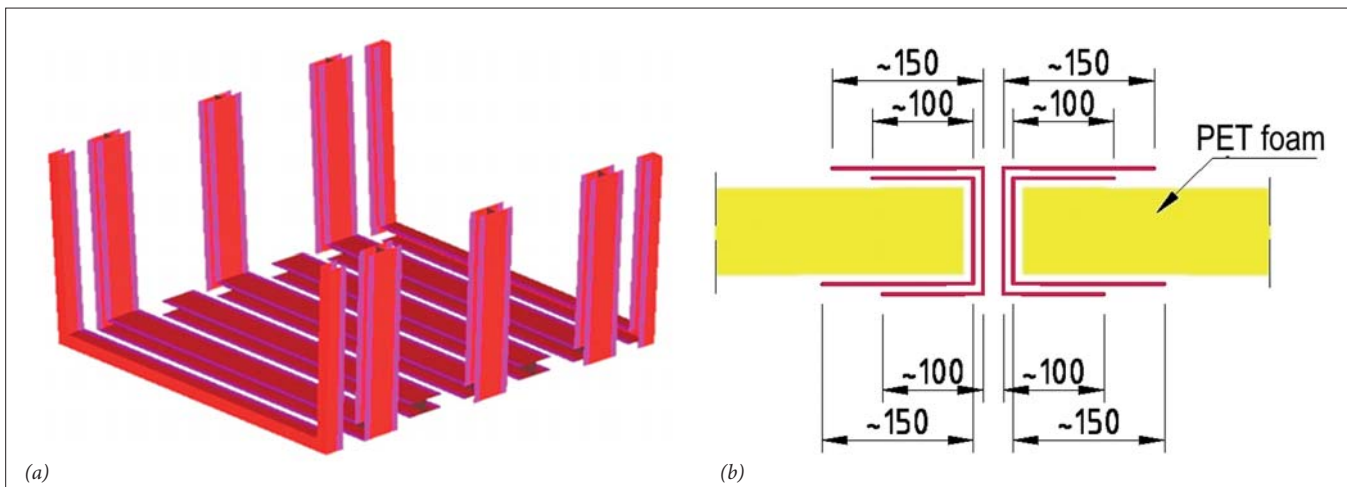


Fig. 10. Ribs used in the segment production

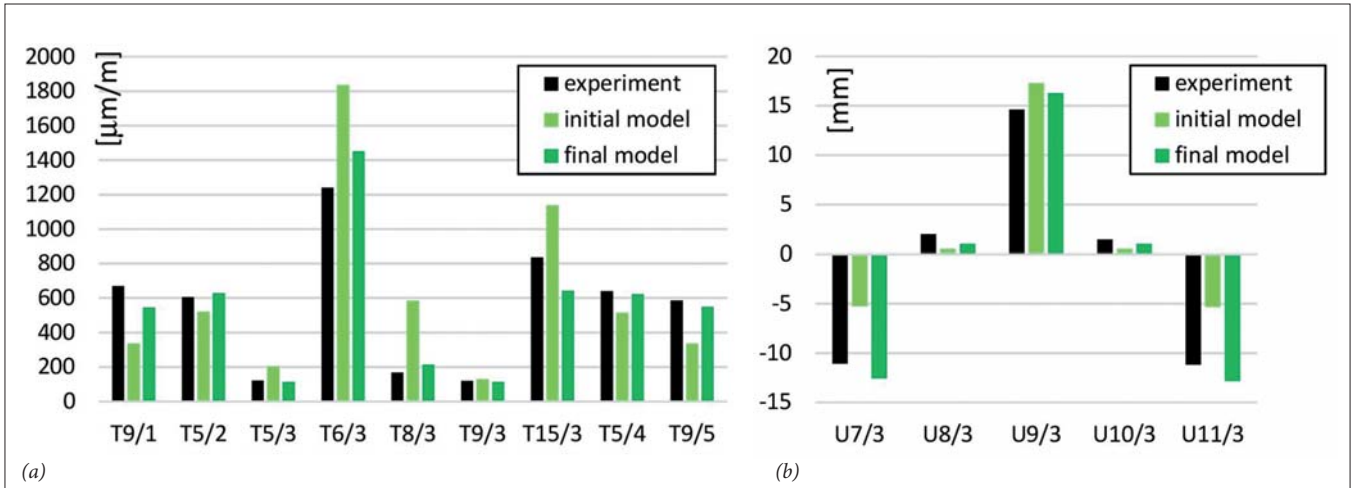


Fig. 11. Comparison of results obtained from experiment and model before and after validation process

Furthermore, Fig. 12–Fig. 23 show graphs of the force-strain and force-displacement relations at chosen points obtained from the experiment and both numerical models. Black and blue lines represent the experiments while light green and dark green show model behaviour before and after the validation process, respectively. Except increased agreement of received values in model

after validation, the graphs show linear behaviour of the segment under the applied load which confirmed assumptions made before tests.

Finally, a visualization of the deformation of the model after validation is presented in Fig. 24, including strain in transverse (Fig. 24a) and longitudinal (Fig. 24b) directions.

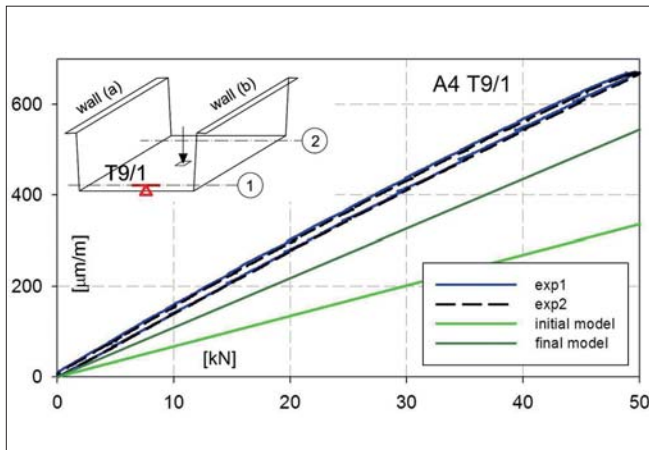


Fig. 12. Strain T9/1 in force function

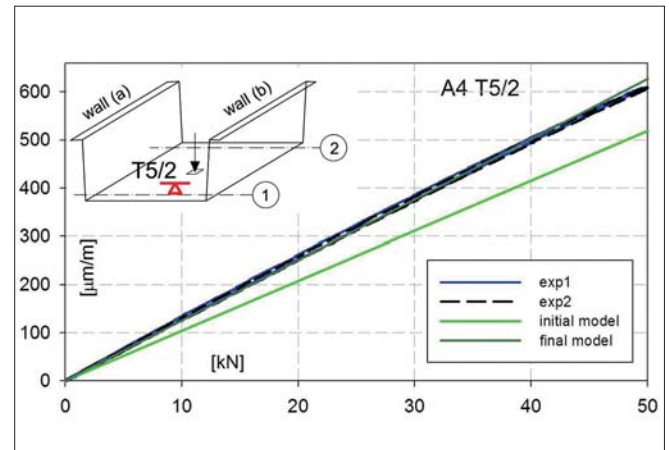


Fig. 13. Strain T5/2 in force function

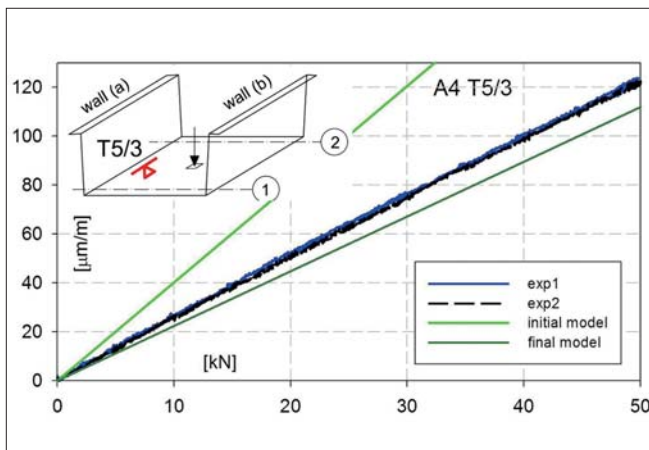


Fig. 14. Strain T5/3 in force function

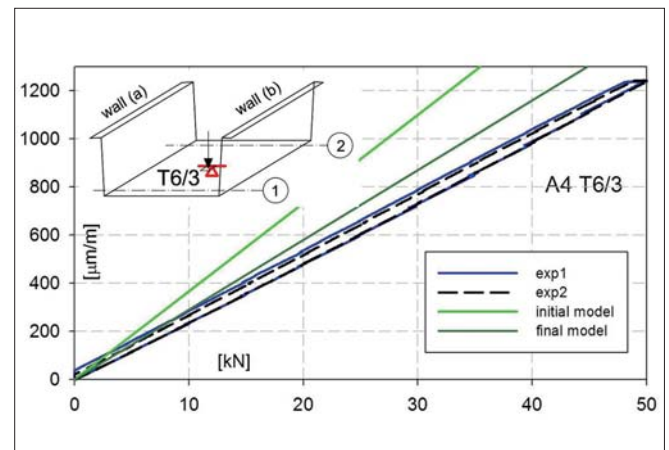


Fig. 15. Strain T6/3 in force function

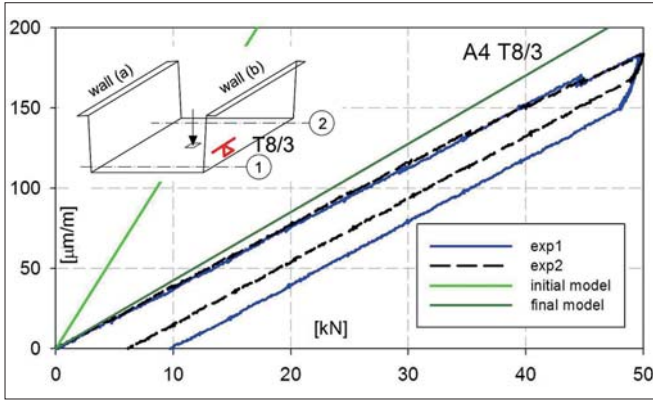


Fig. 16. Strain T8/3 in force function

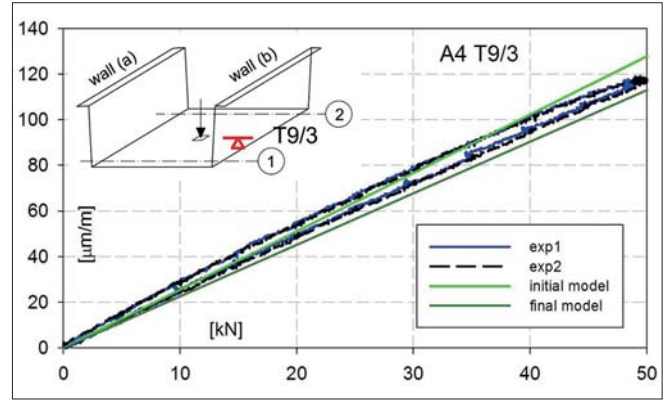


Fig. 17. Strain T9/3 in force function

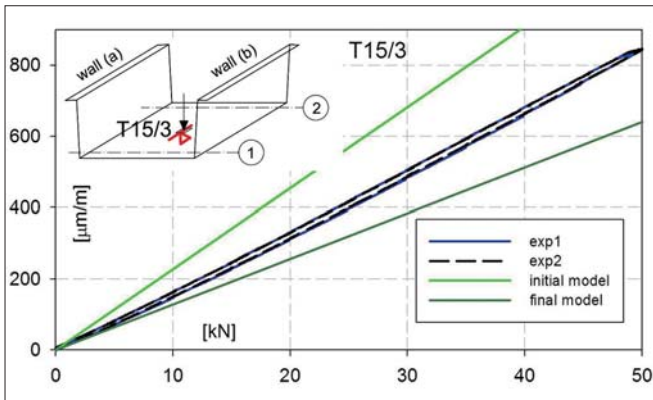


Fig. 18. Strain U15/3 in force function

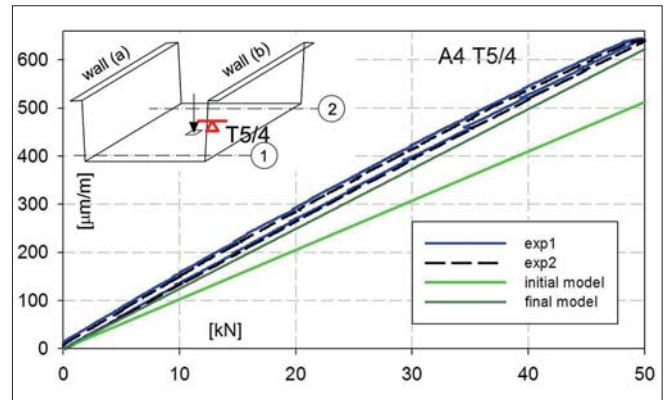


Fig. 19. Strain T5/4 in force function

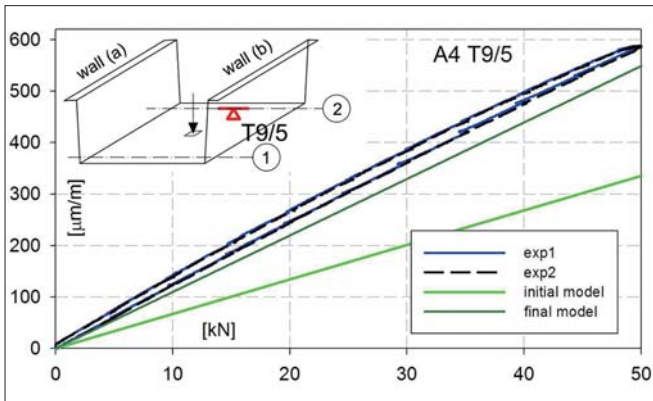


Fig. 20. Strain T9/5 in force function

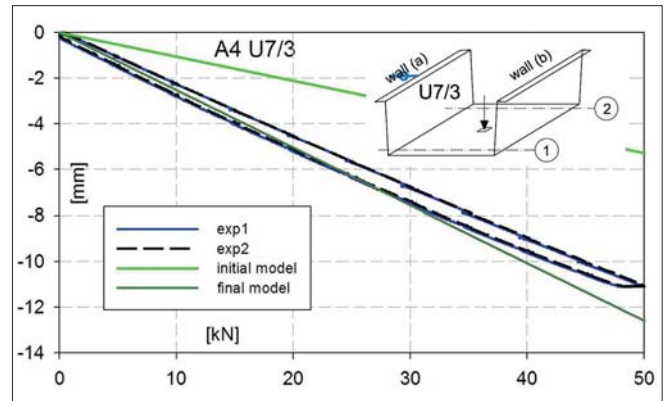


Fig. 21. Displacement U7/3 in force function

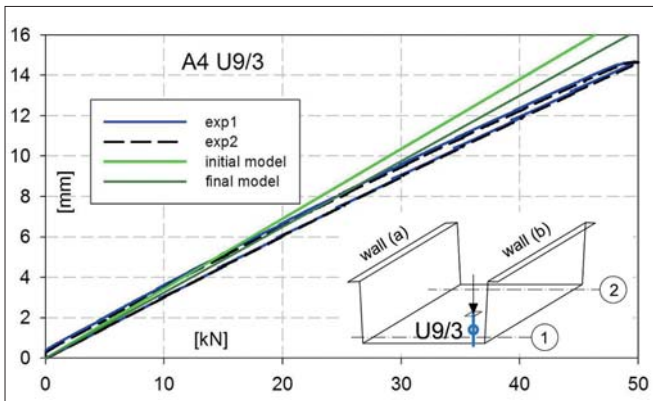


Fig. 22. Displacement T9/3 in force function

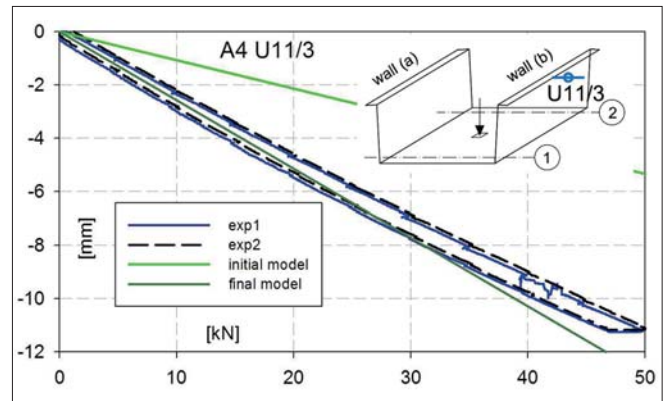


Fig. 13. Displacement U11/3 in force function



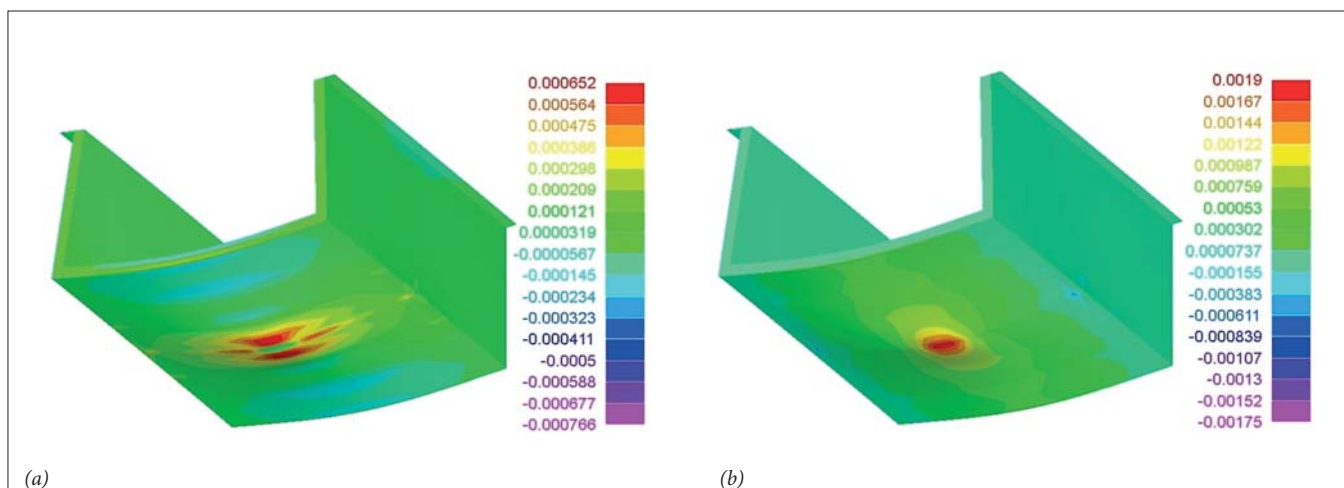


Fig. 24. Segment deformation with strain in (a) transverse direction, (b) longitudinal direction

## CONCLUSIONS

Experiments conducted together with a numerical analysis of the segment allow us to determine behaviour of the structure under applied load. The information obtained from the first comparison instigated some modifications of the numerical model which are shown in the paper. Comparisons after the validation show increased agreement of results which allowed us to extend the numerical model to the size of the target designed composite footbridge and conduct a numerical analysis of it, which was necessary in the design process and in preparation for experiments which were planned to be carried out within the FOBRIDGE project. The experiments were conducted on campus at the Gdansk University of Technology [4, 5].

Despite some differences in obtained results (relative error up to 30% in one sensor), the comparison of results showed the correctness of assumptions made at the stage of building a numerical model of the segment: i.e., the sandwich structure could be modelled using a hybrid method, with shell faces and a solid core. Moreover, the conducted analysis shows that multi-layered laminates can be modelled by means of the ESL approach using FOSD theory. This approach gives satisfying results with sufficient accuracy and is effective.

The presented analysis, which consists of validation of a computational model – just one stage in the design process of a composite bridge – could be enriched by the use of more sophisticated numerical analysis, such as sensitivity analysis [9] or optimization [8].

## ACKNOWLEDGMENTS

This project is supported by the statutory activity No 034161 of the Ministry of Science and Higher Education of Poland. The study was also supported by the National Centre for Research and Development, Poland, grant no PBS1/B2/6/2013.

## REFERENCES

1. Babuska I., Tinsley Oden J. (2004): *Verification and Validation in Computational Engineering and Science: Basic Concepts*, Comput. Methods Appl. Mech. Engrg. 193, 4057–4066.
2. Chróścielewski J., Ferenc T., Mikulski T., Miśkiewicz M., Pyrzowski Ł. (2019): *Numerical Modeling and Experimental Validation of Full-Scale Segment to Support Design of Novel GFRP Footbridge*, Composite Structures, 213, 299–307, DOI: 10.1016/j.compstruct.2019.01.089.
3. Chróścielewski J., Klasztorny M., Romanowski R., Barnat W., Małachowski J., Derewońko A., et al. (2015): *Badania eksperymentalne identyfikacyjne kompozytu. Raport z realizacji podzadania*, 5.1 WAT (internal report), Warsaw.
4. Chróścielewski J., Miśkiewicz M., Pyrzowski Ł., Rucka M., Sobczyk B., Wilde K. (2018): *Modal Properties Identification of a Novel Sandwich Footbridge – Comparison of Measured Dynamic Response and FEA*, Composites Part B, 151, 245–255.
5. Chróścielewski J., Miśkiewicz M., Pyrzowski Ł., Sobczyk B., Wilde K. (2017): *A Novel Sandwich Footbridge – Practical Application of Laminated Composites in Bridge Design and In Situ Measurements of Static Response*, Composites Part B, 126, 153–161.
6. Chróścielewski, J., Miśkiewicz, M., Pyrzowski, Ł., Wilde, K. (2017): *Composite GFRP U-Shaped Footbridge*, Polish Maritime Research, 24(s1), doi:10.1515/pomr-2017-0017.
7. Correia, J. R. (2014): *Fibre-Reinforced Polymer (FRP) Composites*, Materials for Construction and Civil Engineering, 501–556. doi:10.1007/978-3-319-08236-3\_11.
8. Ferenc T., Mikulski T. (2020). *Parametric Optimization of Sandwich Composite Footbridge with U-shaped Cross-Section*,

Composite Structures, 246 (2020) 112406, doi: 10.1016/j.compstruct.2020.112406.

9. Ferenc T., Pyrzowski Ł., Chróścielewski J., Mikulski T. (2018): *Sensitivity Analysis in Designing Process of Sandwich U-Shaped Composite Footbridge*, Shell Structures: Theory and Applications, 4, 413–416, doi:10.1201/9781315166605-94.
10. Fotopoulos K.T., Lampeas G.N., Flasar O. (2019): *Development of an Impact Damage Model for Medium and Large Scale Composite Laminates Using Stacked-Shell Modeling: Verification and Experimental Validation*, Composite Structures, 229, 111386, DOI: 10.1016/j.compstruct.2019.111386.
11. Klasztorny M., Nycz D., Labuda R. (2018): *Modelling, Simulation and Experimental Validation of Bend Tests on GFRP Laminate Beam and Plate Specimens*, Composite Structures 184, 604–612, DOI: 10.1016/j.compstruct.2017.10.046.
12. Kurpińska M., Ferenc T. (2017): *Application of Lightweight Cement Composite with Foamed Glass Aggregate in Shell Structures*, Shell Structures: Theory and Applications Volume 4, DOI: 10.1201/9781315166605-127.
13. Nelson S., Hanson A., Briggs T., Werner B. (2018): *Verification and Validation of Residual Stresses in Composite Structures*, Composite Structures 194, 662–673, DOI: 10.1016/j.compstruct.2018.04.017.
14. Siwowski, T., Kaleta, D., Rajchel, M. (2018): *Structural Behaviour of an All-Composite Road Bridge*. Composite Structures, 192, 555–567, doi:10.1016/j.compstruct.2018.03.042.
15. Pyrzowski Ł. (2018): *Testing Contraction and Thermal Expansion Coefficient of Construction and Moulding Polymer Composites*, Polish Maritime Research, 25(s1), 151–158, doi: 10.2478/pomr-2018-0036.
16. Wiczenbach T., Ferenc T., Pyrzowski Ł., Chróścielewski J. (2019): *Dynamic Tests of Composite Footbridge Segment—Experimental and Numerical Studies*, MATEC Web of Conferences, 285, 00021, DOI: 10.1051/matecconf/201928500021.
17. Zhang W., Liu Y., Luo H., Xue G., Zhang J. (2016): *Experimental And Simulative Study On Accumulator Function in the Process of Wave Energy Conversion*, Polish Maritime Research, 23(3), 79–85, DOI: 10.1515/pomr-2016-0035.
18. Zhang Y., Zhang X., Chang X., Wu Q. (2017): *Experimental and Optimization Design of Offshore Drilling Seal*, Polish Maritime Research, 24, 72–78, DOI: 10.1515/pomr-2017-0107.

## CONTACT WITH THE AUTHORS

### **Tomasz Ferenc**

*e-mail: tomasz.ferenc@pg.edu.pl*  
Gdansk University of Technology  
Faculty of Civil and Environmental Engineering  
Narutowicza 11/12, 80-233 Gdańsk  
**POLAND**

### **Tomasz Mikulski**

*e-mail: tomasz.mikulski@pg.edu.pl*  
Gdansk University of Technology  
Faculty of Ocean Engineering and Ship Technology  
Narutowicza 11/12, 80-233 Gdańsk  
**POLAND**